ELSEVIER

Journal of Alloys and Compounds 275–277 (1998) 488–492

Journal of ALLOYS AND COMPOUNDS

Simulation of energy conversion and transfer in CeF_3 after VUV photon absorption

R.A. Glukhov[a,b,*], A.N. Belsky[a], C. Pedrini[b], A.N. Vasil'ev[a]

[a]*SRL, Faculty of Physics, Moscow State University, 119899 Moscow, Russia*
[b]*LPCML, UMR 5620 CNRS -Universite Lyon I, 43, bd. du 11 Nov. 1918, 69622, Villeurbanne Cedex, France*

Abstract

A Monte-Carlo simulation scheme developed on the basis of the polarization approximation for electron cascade is applied for the investigation of mechanisms of energy conversion in CeF_3 starting from VUV photon absorption and lasting untill the thermalization of electronic excitation. The simulation deals not only with electrons in conduction band and holes in valence and core bands but also with excited states of cerium. The profile of the luminescence excitation spectra in the low energy domain strongly depends on the relative position of the 5d, 6s, 4f Ce and 2p F states. © 1998 Elsevier Science S.A.

Keywords: Monte-Carlo simulation; Electronic structure; Luminescence excitation

1. Introduction

Available simulations of energy relaxation in wide bandgap insulators [1,2] deal with alkaline halides (NaCl, KBr). They use the technique primarily developed for the investigation of the relaxation of high energy particles in the region from mega-electron volts to kilo-electronvolts, the detailed electronic structure being neglected. The number of electron–hole pairs, obtained as a result of such a kind of simulation, is used usually for the estimation of the efficiency of crystals. Being applied to cross-luminescent materials (BaF_2, CsCl) and crystals doped with rare earth ions (CeF_3), the simulation provides the quantum yield of luminescence which is several times larger than the experimental one. One of the reasons for this discrepancy is that the luminescence of these materials is due to certain kinds of excitation [3,4]. For example, in BaF_2 the fast luminescence results from the recombination of a valence electron and a hole of outermost 5p core band, Auger decay being forbidden. The Monte-Carlo simulation shows that the output of 5p holes is substantially less than the number of electron–hole pairs [5].

In the present paper, Monte-Carlo simulation is applied to investigate the role of different processes of energy conversion in CeF_3 at various excitation energies, various types of electronic excitations being accounted for. The influence of the position of the bottom of the conduction band on the output of electronic excitations is studied.

2. Approximations

2.1. Energy band scheme

The energy band scheme of the crystal (see Fig. 1b) was determined on the basis of XPS [4], photoelectron [6] and free atom subshell binding energy data [7]. We assume that the forbidden bandgap E_g equals 10.6 eV. The width of the valence band formed by 2p states of fluoride is 3.5 eV. The outermost core 5p Ce band lies 10.6 eV below the top of the valence band. Compared with alkaline halides, it has the peculiarity of having the 4f Ce band in the forbidden band. It is situated at 4.8 eV from the bottom of the conduction band which originates in the 5d and 6s states of Ce^{3+}. The threshold of 4f–5d transitions E_{4f-5d} is 4.8 eV, and 4f–6s E_{4f-6s} is 6 eV. 4f electrons of cerium are well screened by 5p and 5s electrons, thus the band formed by these electrons in cerium fluoride is narrow (about 0.5 eV) and 4f holes in this partially filled band can hardly move from one ion to another.

We suppose that a direct creation of the exciton is unlikely, as there is no strong excitonic absorption band in the reflectivity spectrum of CeF_3. Therefore we do not take into account excitonic effects (the Urbach tail) at the edge

*Corresponding author.

PII: S0925-8388(98)00378-8

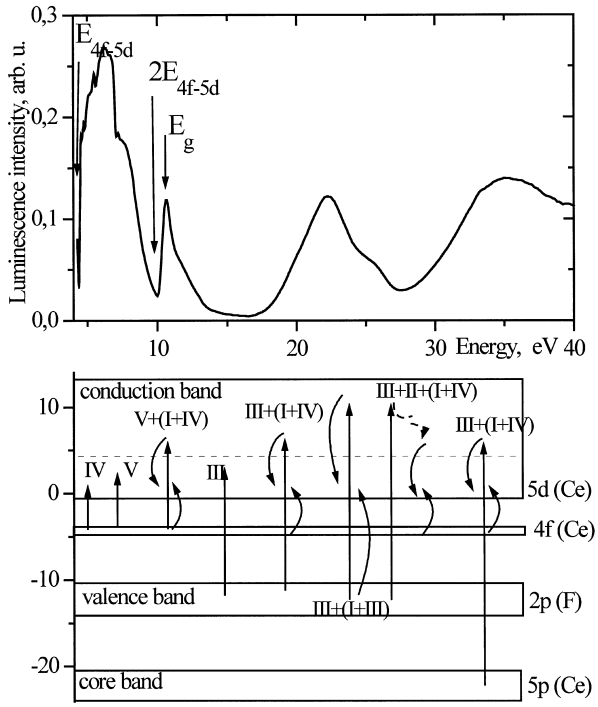

Fig. 1. The experimental yield of luminescence (top) and dominant relaxation processes occuring at various excitation enrgies in CeF_3 (bottom).

of the fundamental absorption. It is possible that the small probability of direct exciton creation is related with the presence of the 4f Ce sub-band [8].

2.2. Creation of primary excitation

The creation of primary excitation is controlled by the imaginary part of the dielectric permittivity which is a function of the energy and wave vector of the photon. In the approximation of the flat core levels, it can be written as a sum of partial contributions of the levels. Then, the probability of the absorption of the photon at a certain level happens to be proportional to the partial imaginary part of the dielectric permittivity corresponding to the level. Following the scheme proposed in [3], it can be described using a model function in which the dependence on the wave vector is omitted:

$$\epsilon_2^{c}(\omega) = A_c\left(\frac{\mathrm{Ry}}{E_c}\right)^2 \frac{a_B^3 N_c}{v} \frac{(z_c-1)^{\alpha_c+1/2}}{z_c^{\beta_c}} \qquad (1)$$

,where E_c is the ionisation energy of the core level, $z_c = \hbar\omega/E_c$, N_c is the number of electrons in the cell of volume v. The constants α_c are estimated from calculations of matrix elements of the transition between the core state and the states which form the bottom of the conduction band. The constants β_c are chosen to fit the dielectric permittivity for energies 30–50 eV above the corresponding thresholds using the atomic photoionization data [9]. The constants A_c are found from the sum rules. Obtained in a such way, dielectric permittivities are adjusted by comparing the experimental absorption coefficient [4,10] with that derived from simulated dielectric permittivities.

2.3. Probabilities of inelastic electron scattering and Auger decay

The probabilities of the electron–electron scattering (see Fig. 2b) and Auger decay for the highest lying core holes, as well as the energy losses of electrons are calculated on the basis of the kinetic equation for electron cascade in the polarization approximation [3,11], the parabolic band approximation being used. In the framework of this approximation, the inelastic electron scattering and Auger processes can be considered as a consequence of the emission and of the absorption of a virtual photon of the polarization field induced by an electron of conduction band or by a hole. Thus the relaxation of the electronic excitation is simply due to elementary processes which can be subdivided into two groups. The former corresponds to the emission of a photon or a phonon:

(I) $e(h) \rightarrow e(h) + \hbar\omega$ emission of a virtual

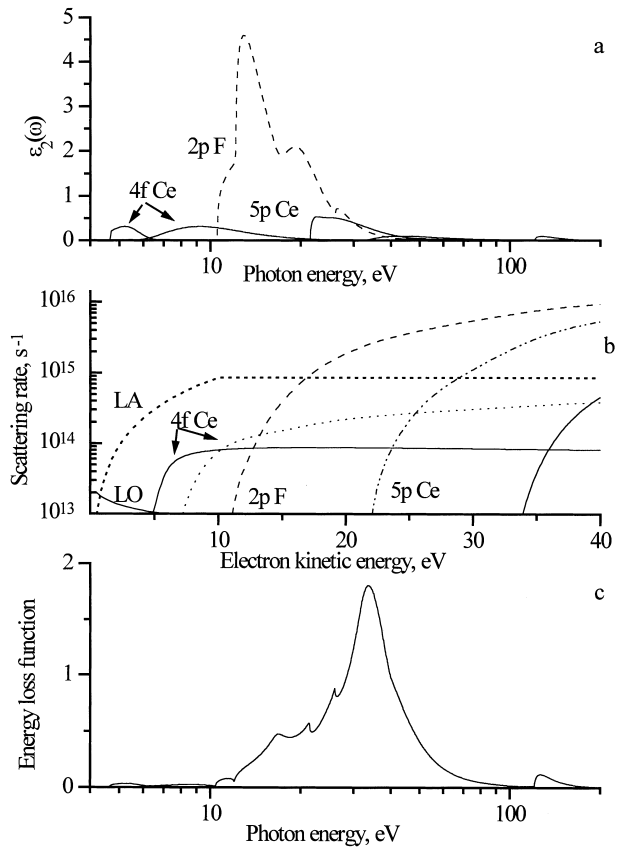

Fig. 2. Simulated (a) partial imaginary part of dielectric permittivities, (b) scattering rate for an electron vs. its kinetic energy and (c) energy loss function for CeF_3.

photon by an electron (hole),

(II) $e(h) \rightarrow e(h)+\hbar\Omega$ emission of a phonon by an electron (hole).

The second one corresponds to a photon absorption:

(III) $\hbar\omega+(v \text{ or } c \text{ band}) \rightarrow e+h$ absorption of a virtual photon from the valence or core band,

(IV) $\hbar\omega+Ce^{3+} \rightarrow (Ce^{3+})^*$ direct excitation of cerium,

(V) $\hbar\omega+Ce^{3+} \rightarrow Ce^{4+}+e$ ionization of cerium,

where e stands for an electron of the conduction band, h is for a hole, $\hbar\omega$ is a virtual or real photon, $\hbar\Omega$ is a phonon.

The interaction with optical phonons is treated with the Fröhlich Hamiltonian. Acoustic phonons are included using the deformation potential theory [12]. The rate for electron–electron scattering is given by the formulae [3]:

$$\frac{1}{\tau(E)}=\frac{e^2\sqrt{2m_e}}{\pi\hbar\sqrt{E-E_g}}\int_0^{E/\hbar} d\omega\ \mathrm{Im}\left(-\frac{1}{\epsilon(\omega)}\right) \ln\frac{\sqrt{E-E_g}+\sqrt{E-E_g-\hbar\omega}}{\sqrt{E-E_g}-\sqrt{E-E_g-\hbar\omega}} \quad (2)$$

.The function under the integral of Eq. (2) is the spectral density of the energy distribution of the virtual photon. Since logarithmic multiplier is a smoothly decreasing function of energy, the structure of the distribution is mainly determined by the energy loss function. This function is computed through the imaginary part of dielectric permittivity using Kramers-Krönig transformation (Fig. 2c).

Relative probabilities of (IV) and (V), as functions of photon energy, are chosen to fit the simulated output of $(Ce^{3+})^*$ to the experimental luminescence yield.

For the initial stages of relaxation when energies of the particles are high, the products of scattering events are distributed over a wide energy region, and the scattering probability slightly depends on the energy of initial particles (see Fig. 2b and c). On the contrary, the final stages of inelastic scattering with production of new excitations strongly depends on the relatively small energy of the particles. Near the threshold of inelastic scattering, multiplication of electronic excitation may be inefficient due to a strong channel of phonon emission.

2.4. The simulation algorithm

We use the standard Monte-Carlo approach modified by accounting for Coulomb interaction between separated electron and hole which are weakly screened in wide bandgap insulators. The simulation algorithm consists of the transformation of coordinates and velocities of *EE* in a small time interval $\Delta t=10^{-16}$ s according to Newtonian motion laws, followed by the simulation of probabilities of scattering events after the time step. The number of particles after thermalization are averaged over the ensemble of 500 trials for absorption of the photon.

3. Results and discussion

The luminescence of CeF_3 is attributed to the emission of a photon by the excited cerium. Assuming the quantum efficiency is equal to one, the output of $(Ce^{3+})^*$ represents the luminescence yield of CeF_3. The simulation of the excitation spectrum of CeF_3 was performed for photon energies from 5 eV to 60 eV (Fig. 3).

For energies below E_{4f-6s}, only the direct excitation of 4f–5d transition occurs (process IV). The yield of $(Ce^{3+})^*$ is one. In the region $E_{4f-6s}<h_\nu<2E_{4f-5d}$, ionisation of cerium results in the creation of separated electron–hole pairs (process V+II). As the photon energy increases, the number of $(Ce^{3+})^*$ diminishes while the number of separated electron–hole pairs increases.

Above 9.6 eV, i.e. the first threshold of multiplication $2E_{4f-5d}$, the primary electron has sufficient energy to excite 4f–5d transition (process V+(I+IV)). The number of $(Ce^{3+})^*$ increases until 10.8 eV.

The abrupt decrease in the number of $(Ce^{3+})^*$ and Ce^{4+}

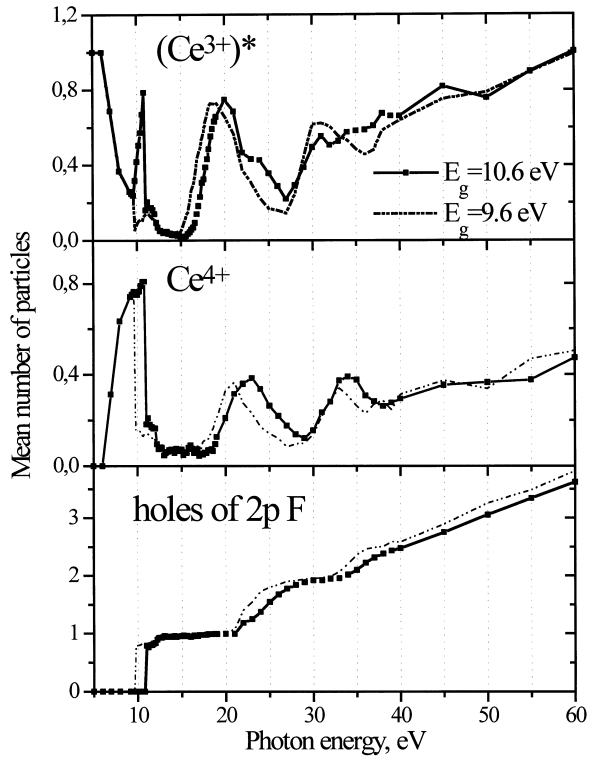

Fig. 3. Number of particles as a result of Monte-Carlo simulation for different energy bandgaps. $E_g=10.6$ eV (solid) and $E_g=9.6$ eV (dashed). Output of $(Ce^{3+})^*$ (a), of Ce^{4+} (b) and holes of 2p (c).

at 11 eV is due to the strong absorption of the photon from the valence band. This channel is strong because of the large number of electrons per elementary cell in 2p F band compared with 4f Ce band (18:1). In spite of that, near the edge of fundamental absorption (up to 13 eV), the contribution of 4f Ce into the dielectric permittivity is not negligible compared with that of 2p F. The small tail in the yield of $(Ce^{3+})^*$ in this region is due to the ionisation of cerium followed by the direct excitation of cerium by secondary electrons.

When h_ν exceeds $E_g + E_{4f-5d}$, a part of the electron is knocked out from the valence band (2p F) which has energy higher than the threshold of inelastic scattering E_{4f-5d}. These electrons may loose their energy by creating additional $(Ce^{3+})^*$ (process III+(I+IV)). Starting from $E_g + E_{4f-6s}$, scattering of the primary electron may lead to ionisation of cerium (process III+(I+V)). When the primary electron arises from the 4f Ce band, a great part of the energy excess over the threshold of inelastic scattering on cerium E_{4f-5d} is acquired by the electron, because the width of the 4f band is small. For the same magnitude of the energy excess ($h_{\nu 1} - E_{4f-5d} = h_{\nu 2} - E_g$), the mean energy of the primary electron arising from the valence band is less than that in the previous case because the width of the valence band is larger than that of 4f Ce and a considerable part of the energy may be acquired by the hole. Therefore the rate of the increase of the number of $(Ce^{3+})^*$ in the region above the second threshold of multiplication $E_g + E_{4f-5d}$ is slower than for the corresponding low energy region above the first threshold $2E_{4f-5d}$. Moreover, above the $E_g + E_{4f-6s}$ the simultaneous rising of the mean number of $(Ce^{3+})^*$ and Ce^{4+} becomes possible and continues up to 20 eV.

The decrease of the yield of either excited or ionised cerium in the region $h_\nu > 2E_g$ is related to the fact that a strong competitive channel of the multiplication of electronic excitations at a valence band appears. But the dip in the yield is not so deep as that in the region from 15 eV to 18 eV because of a larger number of secondary electrons with energy falling into the interval $E_g + E_{4f-5d} < 2E_g$. Either the loss of energy due to electron–phonon interaction (process II) or absorption from the 5p core band (process III+I+IV) provide such electrons.

Starting from 40 eV, the yield of particles becomes linear, the number of valence holes being 3–4 times larger than that of excited cerium and 7 times larger than that of ionized cerium.

In a wide energy region, the yield of excited cerium is less than one. Only at 60 eV it becomes equal to that obtained with a direct excitation of intracenter 4f–5d transitions. The yield of excited cerium turns out to be of the same order of magnitude as the experimental one of the fast luminescence in CeF_3.

There is no unique opinion about the magnitude of the forbidden bandgap E_g of CeF_3 and about the nature of the peak at 10.4 eV in the excitation luminescence spectra. In [13] it was supposed that E_g equals 9.6 eV and the peak was interpreted as an effective energy transfer from excitons of 2p F to Ce. Here we discuss the model for which direct creation of 2p excitons is neglected and the peak at 10.4 eV is associated with a multiplication of electronic excitation above the $2E_{4f-5d}$. A computer experiment with a variation of energy band position was performed. In Fig. 3, the comparative results for different thresholds of transition from valence to conduction band (10.6 eV and 9.6 eV) are shown. It happens that the profile and the magnitude of the peak strongly vary with the bandgap energy. The peak at 10.4 eV and the shoulder at 24 eV in the simulated yield of excited cerium for $E_g =$ 10.6 eV excitation are in good agreement with the peculiarities of the experimental luminescence excitation spectra. In the case with lower threshold, $E_g = 9.6$ eV, these peculiarities were not observed. So the precise measurements of the energy bandgap E_g is necessary to give favour to one of the models proposed.

4. Conclusion

The Monte-Carlo simulation, taking into account the detailed electronic structure of the crystal, shows that the number of excited cerium is 3–4 times less than the total number of electron–hole pairs if the energy transfer from the fluoride sub-system to the cerium one is negligible and the excitation of cerium occurs only through scattering of hot electrons on the cerium sub-system.

The computer experiment can be a good probe for the selection of possible mechanisms of energy conversion in insulators with complex band structure.

Acknowledgements

One of us (R.A.G.) gratefully acknowledges Prof. H. Chermette for providing the access to the computers of Laboratoire de Physico–Chimie Theorique de l'Institut de Physique Nucleaire de Lyon.

References

[1] A. Kikas, M. Elango, Phys. Status Solidi B 130 (1985) 211.
[2] A. Ausmees, M. Elango, A. Kikas, E. Nommiste, J.N. Andersen, R. Nyholm, I. Marttinson, Solid State Commun. 76(12) (1990) 1383–1386.
[3] A.N. Vasil'ev, Nucl. Instr. Meth. B 107 (1996) 165–171.
[4] C. Pedrini, D. Bouttet, C. Dujardin, A.N. Belsky, A.N. Vasil'ev, Proceedings of the International Conference on Inorganic Scintillators and their Applications, SCINT95, Delft University Press, Netherlands, 1996, pp. 103–110.
[5] R.A. Glukhov, A.N. Vasil'ev, Radiat. Def. Eff. 135 (1995) 813–817.
[6] A. Ichikawa, O. Aita, K. Aoki, M. Kamada, K. Tsutsumi, Phys. Rev. B 45 (1992) 3221.

[7] T.A. Carlson, Photoelectron and Auger Spectroscopy, Plenum, New York, 1976, p. 337.
[8] V.N. Makhov, Private communication.
[9] J.-J. Yeh, Atomic Calculation of Photoionization Cross-Sections and Asymmetry Parameters, Gordon and Breach, USA, 1994.
[10] C. Pedrini, B. Moine, J.C. Gacon, Jacqueir, J. Phys. Condens. Matter 4 (1992) 5461.
[11] A.N. Vasil'ev, Mater. Sci. Forum 239–241 (1997) 235–240.
[12] M. Sparks, D.L. Mills, W. Warren, T. Holstein, A.A. Maradudin, L.J. Sham, E. Loh, D.F. King, Phys. Rev. B 24 (1981) 3519.
[13] A.N. Belsky, R.A. Glukhov, P. Martin, V.V. Mikhailin, C. Pedrini, A.N. Vasil'ev, J. Lumin. 72(4) (1997) 96–97.